JOURNAL OF GEOPHYSICAL RESEARCH, VOL. 105, NO. A6, PAGES 12,659–12,666, JUNE 1, 2000

Determination of the abundance of aluminum in the solar wind with SOHO/CELIAS/MTOF

Peter Bochsler
Physikalisches Institut, University of Bern, Bern, Switzerland

Fred M. Ipavich and John A. Paquette
Department of Physics, University of Maryland, College Park

James M. Weygand and Peter Wurz
Physikalisches Institut, University of Bern, Bern, Switzerland

Abstract. The Al/Mg abundance ratio provides an excellent test case for investigating possible fractionation processes among low First Ionization Potential (FIP) elements in the solar wind. Al and Mg are refractory elements; their abundance ratio has been well determined in solar system materials and inferences for the abundance ratio in the solar atmosphere are reliable. Al and Mg are at neighboring masses and have similar charge state properties in the solar corona; hence mass fractionation effects in the solar wind acceleration process and instrumental mass fractionation are minimal. From first observations during two relatively short periods, one recorded in coronal hole associated solar wind, the other in typical interstream solar wind, it is concluded that the solar wind ratio in both regimes is consistent with the solar system ratio. The Al/Mg ratio in interstream solar wind is 0.081±0.012, and in the sample of coronal hole associated solar wind it amounts to 0.076±0.011. A comparison of these results with the solar system ratio of 0.079±0.005 gives no indication for fractionation occurring among low FIP elements in the solar wind.

1. Introduction

The solar Al/Mg ratio is one of the best determined elemental abundance ratios in solar system materials. Both elements, Al and Mg, are refractory and, hence, according to the systematics of *Anders and Grevesse* [1989] this ratio varies little among undifferentiated solar system objects. At the same time, the solar photospheric abundance ratio Al/Mg=0.078±0.016 [*Grevesse and Sauval,* 1998] agrees well with the best meteoritic ratio which is 0.0814±0.0054 [*Kallemeyn and Wasson,* 1981]. This is an important fact because it ensures that this ratio provides a solid baseline for the investigation of the First Ionization Potential (FIP)-dependent element fractionation in different solar wind regimes. Al has a FIP of 5.98 eV, whereas the FIP of Mg is 7.64 eV. The two elements have very similar atomic masses; hence, in a first approximation, mass-dependent effects during particle acceleration in the solar atmosphere and mass-dependent instrumental effects are expected to be negligible. To a better approximation, the mass-dependent behaviour of ^{27}Al can reliably be extrapolated from well-resolved mass spectra of the three abundant and easily detectable isotopes ^{24}Mg, ^{25}Mg, and ^{26}Mg. Similarly, energy per charge properties for both elements are well understood in normal solar wind flows and do not change substantially over the relatively narrow mass per charge range covered by the magnesium isotopes and the only stable, neighboring ^{27}Al isotope.

Solar wind abundances, solar energetic particle (SEP) abundances, and coronal abundances are fractionated relative to solar (photospheric) abundances such that elements with high FIP, i.e., FIP > 10 eV, are depleted relative to elements with low FIP [cf. *Meyer,* 1985]. The depletion factor depends on the properties of the coronal source region. Interstream solar wind which emanates from coronal streamers, generally is depleted by a factor of 3 to 5, whereas the (polar) coronal hole associated solar wind bears a depletion factor of 1.5 to 2 for the high FIP elements. For the case of the solar wind abundances, the depletion factors have heretofore essentially been determined by comparison to the most abundant low FIP elements, i.e., Mg, Si, and Fe. The amount of depletion is known at best to an accuracy of ±30%. Recent optical observations of coronal streamers with SOHO/UVCS [*Raymond et al,* 1997] show no

Paper number 1999JA005085.
0148-0227/00/1999JA005085$09.00

systematic variations among several low FIP elements between the interior of a quiescent streamer center, a quiescent streamer leg, and an active region streamer. For solar energetic particles (SEPs) several other elemental abundances have been determined with good accuracies. SEP determinations give, however, access to coronal abundances in a less direct manner than obtained with solar wind observations because the acceleration process can at times lead to substantial M/Q fractionation [*Breneman and Stone,* 1985; *Reames,* 1998].

The more sophisticated models, which have made an attempt to explain the FIP-dependent elemental fractionation in a quantitative manner, use time-dependent processes to reproduce the observed ion-neutral fractionation. In that respect the Al/Mg abundance ratio is even more interesting since the ionization times of Al and Mg differ by more than an order of magnitude (see Table 2).

2. Instrumental

The mass time of flight (MTOF) sensor is part of the CELIAS experiment onboard SOHO. CELIAS is the result of a joint effort of five hardware institutions under the direction of the Max-Planck-Institute for Extraterrestrial Physics, Garching (prelaunch) and the University of Bern (postlaunch). The University of Maryland was the prime hardware institution for MTOF, the University of Bern provided the entrance system to MTOF, and the Technical University of Braunschweig provided the Digital Processing Unit for CELIAS.

The MTOF sensor consists of a wide energy passband E/Q (energy per charge) filter (WAVE) and an isochronous time of flight spectrometer in a V-type configuration with a resolution $M/\Delta M \sim 100$. The CELIAS experiment has been documented in more detail in a publication by *Hovestadt et al.*[1995]. Details on the MTOF sensor as well as on its operation and calibration can be found in the *Kallenbach et al.* [1997] study. The main purpose of the E/Q filter is to suppress the abundant protons and alpha particles and also to efficiently prevent solar UV from entering into the sensitive parts of the time of flight section. It is cycled in two steps through the E/Q range of solar wind particles, thereby covering all minor species up to Fe. The passband of the E/Q filter at a given voltage setting U_{WAVE} includes a range of approximately $0.3 < E/(QU_{WAVE}) < 1.2$(FWHM). Before entering the time of flight section of the instrument, ions can be accelerated, decelerated, or left unchanged to adapt them to the energy range of the isochronous detection system. The time of flight of a single ion is measured between a start pulse from a microchannel plate detector, triggered by electrons which are released at the passage of the ion through a thin (2.1 $\mu g/cm^2$) carbon foil, and a stop pulse, generated on a position sensitive microchannel plate detector. The mass per charge in an isochronous time of flight mass spectrometer is determined via the relation $m/q \propto t^2$. The charge state distribution of the ions leaving the foil is inferred from a comprehensive series of calibrations [*Gonin et al.,* 1995, and references therein]. The relevant data including data on Al and its multiply charged species are also contained in the thesis of *Gonin* [1995]. In the energy range considered for this work, only a small fraction of particles leaves the carbon foil as doubly or multiply charged species. Doubly charged ions appear at half atomic masses in the time of flight spectra. For instance, $^{54}Fe^{++}$ blends with the $^{27}Al^{+}$ peak, hence, a small correction to the ^{27}Al abundance is necessary. This correction was applied adopting a solar system isotopic composition of solar wind Fe and a solar system Fe/Al abundance ratio for the solar wind. Such an assumption can be justified in view of the fact that both, Fe and Al, are low FIP elements and in view of the smallness of the correction which amounts to typically 6%.

An important ingredient affecting the determination of an abundance ratio is the secondary electron yield of different elements and ions in the start carbon foil. The investigations of *Gonin et al.* [1995] have shown that (at least for small and medium mass elements) no memory of the initial charge state is found after passage through the carbon foil, and that the interaction of the projectile with the backside of the carbon foil essentially determines the properties of the outgoing particles. Since the start pulse is generated in a very similar process by interaction of an outgoing particle with the backside of the carbon foil, it seems reasonable to assume that the start efficiency does not depend on the initial charge state of a particle. It has been shown that the electron yield of different medium mass elements is very similar for a given velocity of projectiles [e.g., *Rothard et al.,* 1990; *Ritzau and Baragiola,* 1998]. Furthermore, the velocity dependence of the electron yield has been carefully calibrated for some medium mass elements and charge states with a spare MTOF sensor unit.

3. Data Selection

From the 3 years of available data since launch of SOHO in December 1995, two relatively short periods were chosen for a detailed analysis. The first period covers approximately 4 days of interstream (IS) solar wind data which were registered from October 31, 1998, through the morning of November 4, 1998. From observations of the proton monitor (CELIAS/PM) [see *Ipavich et al.*, 1998] it is found that very quiet conditions prevailed during the entire period. The proton speed remained within a margin of ±10 around 400 km/s. The thermal speed of the protons was around 30 km/s. The second period considered in this study lasted 15 hours, beginning November 23, 1998 at 2201 UT and ending at November 24, 1302 UT. Conditions in this period can be characterized as typical for coronal hole associated fast streams (CH). Again, rather stable conditions

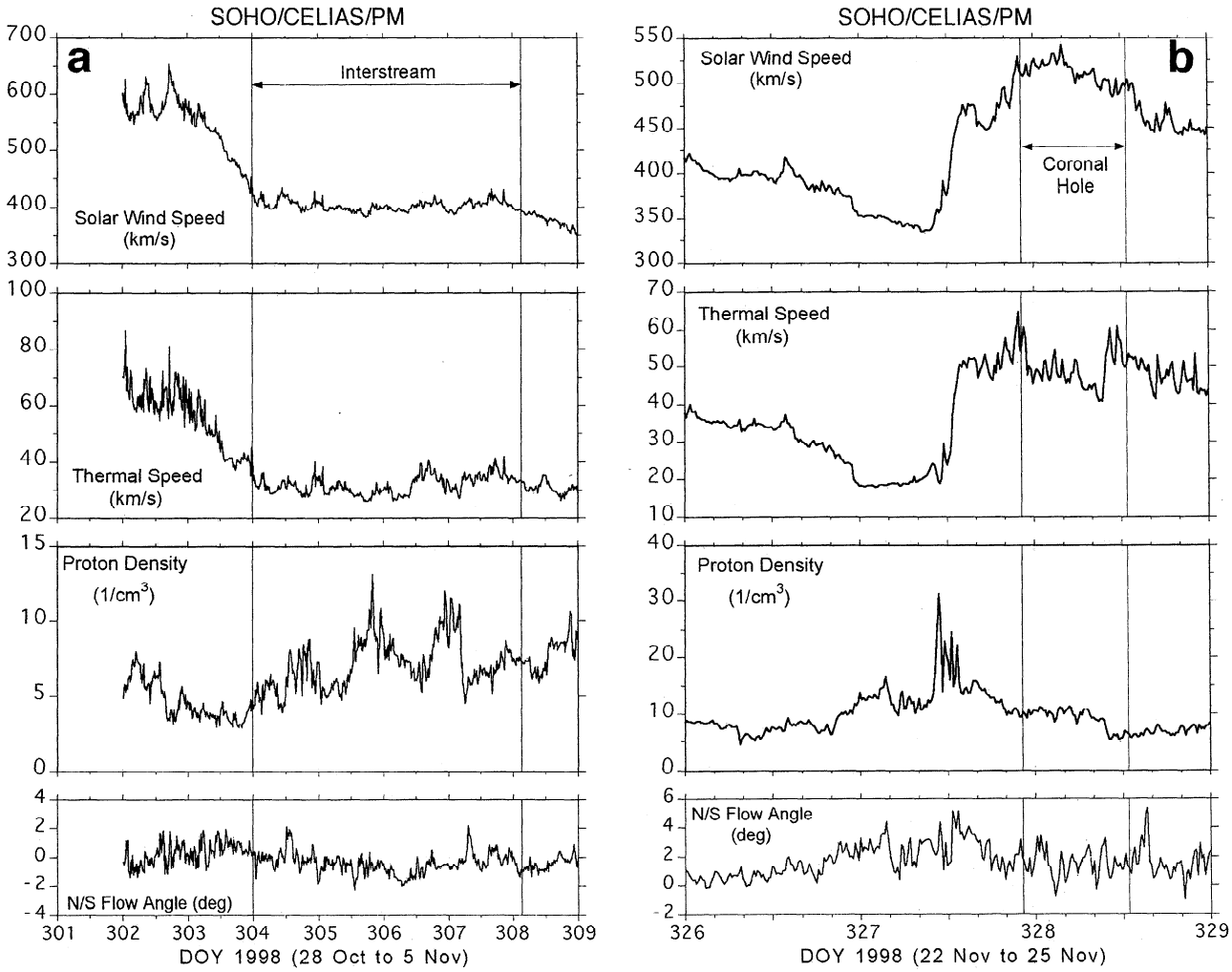

Figure 1. Kinetic solar wind properties of two selected periods (shaded areas) as recorded with the proton monitor (PM) of the CELIAS experiment on SOHO: (a) Interstream solar wind day of year (DOY) 304-307, 1998, and (b) coronal hole associated solar wind on DOY 328, 1998.

prevailed with a solar wind speed of $\sim$ 510 km/s and a proton thermal speed of 50 km/s varying within narrow limits. The relevant solar wind parameters for the two selected periods are illustrated in Figure 1.

4. Data Analysis

The mass spectrum obtained during the IS period is shown in Figure 2, the spectrum for the CH period is in Figure 3. This section contains some details on the data reduction procedures. The observed spectrum was assumed to contain 9 species: ^{20}Ne, ^{21}Ne, ^{22}Ne, ^{23}Na, ^{24}Mg, ^{25}Mg, ^{26}Mg, ^{27}Al, and ^{28}Si superposed to a background count rate with a weak linear dependence on the time of flight. The maximum likelihood fit to the observations was carried out with 17 free parameters. Since the time of flight in an isochronous mass spectrometer is proportional to the square root of the mass of the particles, this proportionality was used to attribute the masses to the times of flight of the peaks in the spectrum, allowing for a small, identical offset for all peaks according to the following expression

$$T_i = (T_{24} - T_{\mathrm{offset}}) \sqrt{\frac{m_i}{m_{24}}}, \qquad (1)$$

where T_i is the nominal time of flight of a species i with nuclear mass m_i, and T_{offset} is the offset of the time of flight. The two free parameters T_{offset}, and T_{24} were used to fix the locations of all 9 species within the selected time of flight range. Two more parameters, b_o and b_1, were used to fit the background count rate over the time of flight range considered:

$$b(T) = b_o + b_1 T. \qquad (2)$$

Each peak was parameterized using a superposition of two Lorentzians and one Gaussian. All peak shapes were kept similar and the relative proportion of the Lorentzians and the Gaussian was kept constant for all 9 peaks. To match the asymmetry of the peaks inherent in isochronous time of flight spectra, two half-

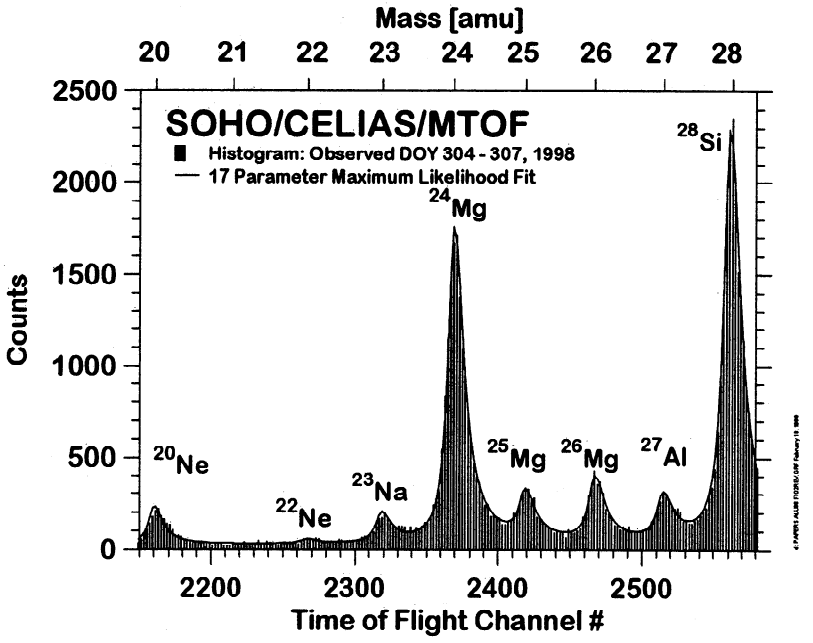

Figure 2. Summed spectrum as recorded during the interstream period from DOY 304-307, 1998. The solid line shows the result of the 17 parameter maximum likelihood fit.

Lorentzians with two different widths were applied to describe the peak shapes. One width of the Lorentzian ($\Gamma_{i,L}$) matches the counts on the left-hand side of the peak i, the other ($\Gamma_{i,R}$), is to match the right-hand side. For the Gaussian a symmetric σ_i was adopted. All widths were assumed to be proportional to the square roots of the masses m_i of the 9 species considered. Thus 4 more free parameters were required to adapt peak widths and the proportion of Gaussians and Lorentzians within the peaks. The remaining 9 parameters were used to fit the peak heights of each species individually. The 17 parameter description of the spectrum is then as follows:

$$\mu(T) = \sum_{T_i>T, i=1}^{9} H_i \left[\left(\frac{\Gamma_{i,L}^2}{(T-T_i)^2 + \frac{\Gamma_{i,L}^2}{4}} \right) \right] + \sum_{T_i>T, i=1}^{9} H_i \left[f e^{-\frac{(T-T_i)^2}{2\sigma_i^2}} \right]$$

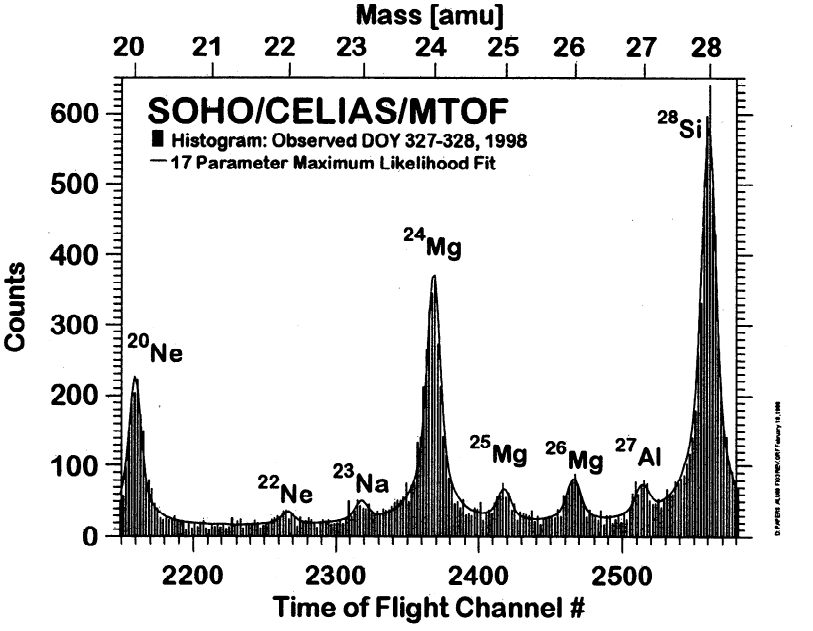

Figure 3. Summed spectrum as recorded during a period of 15 hours of coronal hole asssociated solar wind on DOYs 327 and 328, 1998. The solid line shows the result of the 17 parameter maximum likelihood fit.

$$+ \sum_{T_i \le T, i=1}^{9} H_i \left[\left(\frac{\Gamma_{i,R}^2}{(T-T_i)^2 + \frac{\Gamma_{i,R}^2}{4}} \right) \right]$$

$$+ \sum_{T_i \le T, i=1}^{9} H_i f \left[e^{-\frac{(T-T_i)^2}{2\sigma_i^2}} \right] + b_o + b_1 T. \quad (3)$$

In order to determine the 17 free parameters (among them the 9 peak heights H_i of interest) a maximum likelihood criterion was applied to match the observed count numbers n(T) and the fitted curve $\mu(T)$ over the full range of T values considered. The count numbers $n(T)$ at a given T for an expectation value $\mu(T)$ are distributed according to Poisson statistics:

$$p\,[n(T)|\mu(T)] = \frac{\mu(T)^{n(T)} e^{-\mu(T)}}{n(T)!}. \quad (4)$$

The negative logarithm of the likelihood

$$\begin{aligned} F &= -\sum_T ln[p(n(T)|\mu(T))] \\ &= -\sum_T n(T) ln(\mu(T)) + \sum_T \mu(T) + \sum_T ln[n(T)!] \end{aligned} \quad (5)$$

has to be minimized by varying all 17 free parameters. This procedure was carried out with the search routine E04KDF from the program library of the Numerical Algorithm Group (NAG). Usually, rapid convergence is achieved, indicating that the problem has a unique solution. The results of the seventeen parameter maximum likelihood fits are shown as solid lines over the histograms of recorded data in Figures 2 and 3.

Finally, a forward model was used to simulate count rates per unit element abundances at the relevant solar wind conditions. Owing to the width of the E/Q passband of MTOF it is not possible to differentiate between different charge states of minor species. However, for the instrument settings chosen for this investigation, the relative sensitivity for Al relative to Mg varies only little over the expected charge state distributions of Al and Mg. To derive realistic charge state distributions of Al, Mg, and Si, the time-dependent system of differential equations of ionization and recombination using the rates of *Arnaud and Rothenflug* [1985] was solved. The radially varying local coronal conditions were inferred from ion velocity and electron temperature profiles. This procedure also reproduced realistic charge state distributions of Fe, for both, coronal hole and interstream conditions. The result confirmed that while Mg^{10+} is the dominant species among the Mg ions, Al is distributed over a relatively wide M/Q range going from 4.5 (Al^{6+}) to 2.45 (Al^{11+}). Nevertheless, the estimation of the charge state distribution for Mg and Al is rather insensitive to the assumed coronal conditions. Whatever the coronal conditions are, M/Q (and E/Q) of Al ions spread over a fairly wide parameter range which yields in total a variability of instrument sensitivity within narrow bonds. The forward model also includes a detailed physical description of all parts of the MTOF sensor, i.e., the E/Q passband properties of the WAVE entrance system, the charge conversion efficiency, scattering properties, the start electron yield of the carbon foil at the entrance of the TOF sector, and the stop detection efficiency of the TOF sector. The model was tested against instrument calibration data for Fe and O ions which had previously been obtained with the flight model of MTOF and a spare unit of MTOF at the calibration facilities of the University of Bern.

Table 1. Al/Mg Abundance Ratios in Solar Particles and in the Solar System

	Ratio
Interstream solar wind	0.081±0.012
Coronal hole associated wind	0.076±0.011
SEPs[a](Gradual events)	0.079±0.009
Meteoritic[b]	0.0814±0.0054
Solar System[c]	0.079±0.005

[a] SEPs, Solar Energetic Particles as reviewed by *Reames* [1998].

[b] Carbonaceous chondrites of type I [*Kallemeyn and Wasson*, 1981].

[c] Inferred from meteoritic and photospheric determinations [*Anders and Grevesse*, 1989].

5. Results

The Al/Mg ratios for the two selected periods are presented in Table 1. Both periods yield elemental ratios which are consistent with the meteoritic and solar system ratios as given in the compilation of *Anders and Grevesse* [1989]. The estimated two sigma relative uncertainties of the flux ratios for the two events amount presently to ±15%. These estimates include the effect of the uncertainty in the charge state abundances due to instrumental discrimination of Q/M for Al and Mg (±7%), the uncertainty in the elemental discrimination due to release of start electrons (±7%), the uncertainty in elemental discrimination due to charge state conversion in the carbon foil, (±5%), and ±7% for the uncertainty in elemental discrimination in the stop detection efficiency. The estimated uncertainty of the contribution of doubly charged ^{54}Fe on $^{27}Al^+$ and of the background correction amounts to less than ±5%. All these uncertainties are rather conservative estimates of independent uncertainties which can be added quadratically. An independent check for mass discriminating effects can be obtained from the determinations of the isotopic abundance ratios of Mg which appears to be less than 10% based on the assumption that the solar

Table 2. Atomic Properties of Elements

	First Ionization Potential eV	First Ionization Time[a] s	Collision Radius Neutral Species With H, Å
He	24.587	227	1.56
Ne	21.565	81	1.75
N	14.534	68	2.11
H	13.598	65	-
O	13.618	62	2.26
Ar	15.760	50	2.07
C	11.260	27	2.34
Kr	14.000	20.3	2.17
S	10.360	11.6	2.58
Xe	12.130	10.1	2.35
Na	5.139	1.5[b]	3.5[c]
Si	8.151	1.1	2.91
Fe	7.902	0.91	3.09
Mg	7.646	0.78	3.09
Ca	6.113	0.70	3.64
Al	5.986	0.02[b]	3[c]

[a] *Marsch et al.* [1995].
[b] See *Geiss* [1998] (electron temperature of 6000 K).
[c] Interpolated from atomic systematics.

wind Mg isotopic abundances truly reflect solar system abundance ratios.

6. Discussion

Table 2 is a compilation of first ionization potentials and chromospheric ionization times of elements previously measured in the solar wind. Under photospheric conditions Al is virtually completely ionized (as are several other low FIP elements) and it has by far the shortest ionization time of the more abundant elements; hence it provides an important test case for models explaining solar wind and coronal element fractionation and the so-called FIP effect. A systematic and critical discussion of theoretical FIP models is beyond the scope of this paper. The absence of discrimination among low FIP elements with very different ionization times poses a problem to some of the steady state scenarios as has already been pointed out, e.g., by *Marsch et al.* [1995], *Geiss* [1998], and *Schwadron et al.* [1999]. The magnetic structures in the diffusion model of *Geiss and Bochsler* [1985] and of *von Steiger and Geiss* [1989] retain all ionized species equally and, hence, avoid discrimination among the low FIP elements. Similarly, from the model of *Wang* [1996] one would not expect fractionation among the low FIP elements since in his picture all ions are efficiently pushed into the corona. On the other hand, *Marsch et al.* [1995] and *Peter* [1996] essentially make an attempt to explain the FIP effect as a consequence of atomic properties only. For instance, *Marsch et al.* [1995] use a particularly simple expression which succeeds to quantitatively reproduce the observed interstream abundances of the most abundant species:

$$f_{jk} \simeq \frac{r_{kH}}{r_{jH}} \sqrt{\frac{\tau_k}{\tau_j}} \left(\frac{A_j + 1}{A_j} \frac{A_k}{A_k + 1} \right)^{1/4}, \qquad (6)$$

where f_{jk} is the fractionation factor relating the abundance ratio of two elements j and k relative to their photospheric ratio, r_{iH} is the collisional radius of the neutral species i with neutral hydrogen, A_i is the atomic mass, and τ_i is the standard ionization time of species i. *Peter* [1996] includes a transit time of particle flow through the chromosphere. His model even succeeds to reproduce the observed difference between FIP fractionation in low-speed solar wind and in high-speed streams. The model also produces a very flat low FIP fractionation plateau, however, it must fail to reproduce the absence of fractionation of Al relative to Mg as observed in the solar wind and in solar energetic particles [e.g., *Reames* , 1998] . Figure 4 (open circles) illustrates the prediction of (6). While it roughly reproduces the fractionation pattern for intermediate and slowly ionizing elements it fails to reproduce the observed solar wind abundances (squares and diamonds) of the newly determined, quickly ionizing elements, a limitation which has been pointed out specifically for the case of Al in the *Marsch et al.* [1995] study. Formally, one might modify (6) to

$$f_{jk} \simeq \frac{r_{kH}}{r_{jH}} \sqrt{\frac{\max(\tau_{\rm stream}, \tau_{\rm k})}{\max(\tau_{\rm stream}, \tau_{\rm j})}} \left(\frac{A_j + 1}{A_j} \frac{A_k}{A_k + 1} \right)^{1/4}, \qquad (7)$$

with $\tau_{\rm stream}$ representing a "replenishment time" of either 25 s for coronal hole associated solar wind or of 4 s for interstream solar wind.

The newly determined Al/Mg ratio confirms the flatness of the low FIP plateau over ionization times differing by more than an order of magnitude. Considering also the new solar wind Na/Mg ratio [*Ipavich et al.*, 1999] leads to the same conclusion, however, including ionization times which differ even by two orders of magnitude. Clearly, this demonstrates that while the ionization time seems to be a crucial parameter to explain the abundances of intermediate and slowly ionizing species, it plays no essential rôle in shaping solar wind abundances of elements with first ionization times (FITs) shorter than a few seconds. Apparently the solar atmosphere supplies elements with low FIPs without discrimination according to FIPs or FITs into the solar wind, or in other words, despite the fact that the main gas, hydrogen, is a high FIP element in this picture, it seems that the corona is depleted in high FIP elements, rather than enriched in low FIP elements. This result

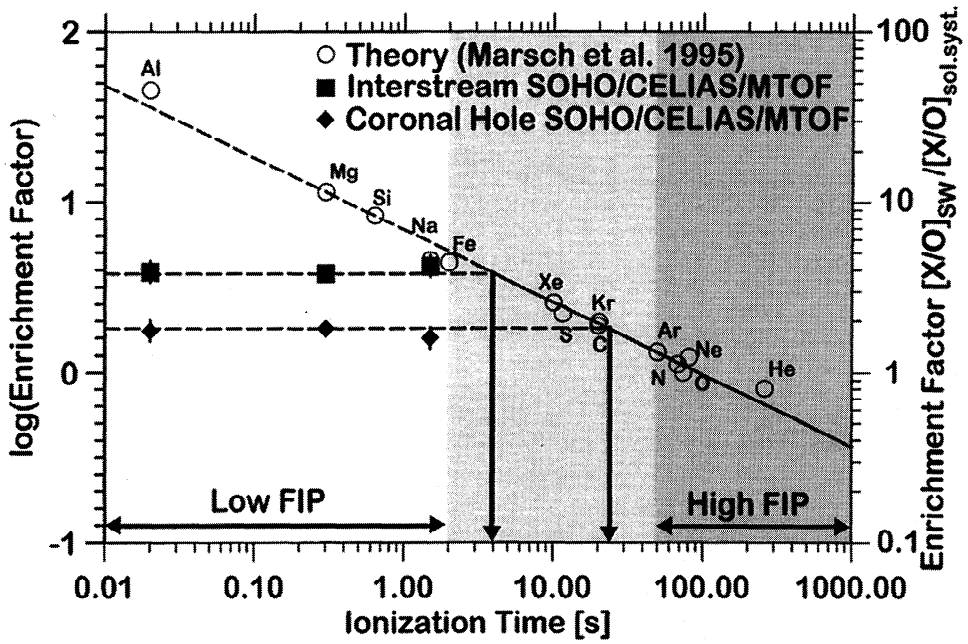

Figure 4. Enrichment factors of solar wind elements as function of the chromospheric ionization time. Open circles indicate the result of the simple formula given by *Marsch et al.* [1995], and using the atomic data as listed in Table 2. The recent determinations of Al (this work) and of Na [*Ipavich et al.*, 1999] are shown as solid black squares for the interstream solar wind and as solid black diamonds for the coronal hole associated observations. Note that the observational Mg abundances have arbitrarily been set to 4 (interstream solar wind) or 2 (coronal hole associated wind) respectively (see, e.g., *von Steiger et al.* [1997] for factually determined solar wind Mg/O ratios). While the equilibrium formula provides a fairly good approximation to the observed abundances of elements with intermediate and long ionization times, it fails to reproduce abundances for elements with ionization times shorter than 25 s (coronal hole associated wind) and 2 s (interstream solar wind). The difference may be (partly) due to different UV radiation levels in the source regions feeding the different solar wind flows.

supports a picture similar to the one of *von Steiger and Geiss* [1989] or of *Wang* [1996] in which some process supplies species, once they are ionized, without further discrimination into the solar wind.

In conclusion, and considering the improved precision of abundance determinations now achieved with CELIAS/MTOF, for future work, it is necessary to verify the flatness of the FIP plateaus for solar wind abundances. If the high FIP element plateau can be established, it seems feasible to derive some solar elemental abundances, especially those of volatile and moderately volatile species, from solar wind abundance ratios with a precision comparable or better than the one derived from presently available photospheric data.

Acknowledgments. The authors are grateful to all the individuals who participated in the design, the construction, and the calibration of CELIAS/MTOF; they thank Scott Lasley for assistance in the data analysis. Edward Anders and Hartmut Holweger contributed helpful advice concerning the choice of reliable solar system elemental abundances. The paper benefitted from a thorough and expeditious review by Thomas Zurbuchen and George Ho. This work was supported by the PRODEX program of ESA and the Swiss National Science foundation, and by NASA under grants NAG5-2754 and NAG5-7678.

Janet G. Luhmann thanks Thomas Zurbuchen and George C. Ho for their assistance in evaluating this paper.

References

Anders, E., and N. Grevesse, Abundance of the elements: Meteoritic and solar, *Geochim. Cosmochim. Acta, 53,* 197-214, 1989.

Arnaud, M. and R. Rothenflug, An updated evaluation of recombination and ionization rates. *Astron. Astrophys. Suppl. Ser., 60,* 425-457, 1985.

Breneman, H.H., and E.C. Stone, Solar coronal and photospheric abundances from solar energetic particle measurements. *Astrophys. J., 299,* L57-L61, 1985.

Geiss, J., Constraints on the FIP mechanisms from solar wind abundance data, in *Solar Composition and Its Evolution - From Core to Corona, Proceedings of an ISSI Workshop 26-30 January 1998, Bern, Switzerland,* edited by C. Fröhlich, M.C.E. Huber, S.K. Solanki, and R. von Steiger, pp. 241-252, Kluwer Acad., Norwell, Mass., 1998.

Geiss, J., and P. Bochsler, Ion composition in the solar wind in relation to solar abundances, in *Rapports isotopiques dans le système solaire,* pp. 213-228, Cépaduès-Editions, Paris, 1985.

Gonin, M., Ein semiempirisches Modell des Ladungsaustausches von niederenergetischen Ionen beim Durchgang durch dünne Folien zur Eichung von isochronen Flugzeit-Massenspektrometern, thesis: Univ. of Bern, Bern, Switzerland, 1995.

Gonin, M., R. Kallenbach, P. Bochsler, and A. Bürgi, Charge exchange of low energy particles passing through thin carbon foils: Dependence on foil thickness and charge state yields of Mg, Ca, Ti, Cr. and Ni, *Nucl. Instrum. Methods B, 101*, 313-320, 1995.

Grevesse, N., and A.J. Sauval, Standard solar composition, in *Solar Composition and Its Evolution - From Core to Corona, Proceedings of an ISSI Workshop 26-30 January 1998, Bern, Switzerland,* edited by C. Fröhlich, M.C.E. Huber, S.K. Solanki, and R. von Steiger, pp. 133-141, Kluwer Acad., Norwell, Mass., 1998.

Hovestadt, D., et al., CELIAS - Charge, Element and Isotope Analysis System for SOHO, *Sol. Phys., 162*, 441-481, 1995.

Ipavich, F.M., P. Bochsler, S.E. Lasley, J.M. Paquette, and P. Wurz, The abundance of sodium in the solar wind as measured by SOHO/CELIAS/MTOF, *Eos Trans. AGU, 80*, 256, 1999.

Ipavich, F.M., et al., Solar wind measurements with SOHO: The CELIAS/MTOF Proton Monitor, *J. Geophys. Res., 103*, 17,205-17,214, 1998.

Kallemeyn, G.W., and J.T. Wasson, The compositional classification of chondrites, I, The carbonaceous chondrite groups, *Geochim. Cosmochim. Acta, 45*, 1216-1230, 1981.

Kallenbach, R., et al., Isotopic composition of solar wind neon measured by CELIAS/MTOF on board SOHO, *J. Geophys. Res., 102*, 26,895-26,904, 1997.

Marsch, E., R. von Steiger, and P. Bochsler, Element fractionation by diffusion in the solar chromosphere, *Astron. Astrophys., 301*, 261-276, 1995.

Meyer, J.-P., The baseline composition of solar energetic particles, *Astrophys. J. Suppl. Ser., 57*, 151-171, 1985.

Peter, H., Velocity-dependent fractionation in the solar chromosphere, *Astron. Astrophys. 312*, L37-L40, 1996.

Raymond, J.C., et al., Composition of coronal streamers from the SOHO Ultraviolet Coronagraph Spectrometer, *Sol. Phys. 175*, 645-665, 1997.

Reames, D.V., Solar energetic particles: Sampling coronal abundances, *Space Sci. Rev., 85*, 327-340, 1998.

Ritzau, S.M., and R.A. Baragiola, Electron emission from carbon foils induced by keV ions, *Phys. Rev. B., 58*, 2529-2538, 1998.

Rothard, H., K. Kroneberger, A. Clouvas, E. Veje, P. Lorenzen, N. Keller, J. Kemmler, W. Meckbach, and K.-O. Groeneveld, Secondary-electron yields from thin foils: A possible probe for the electronic stopping power of heavy ions, *Phys. Rev. A. 41*, 2521-2535, 1990.

Schwadron, N.A., L.A. Fisk, and T. Zurbuchen, Elemental fractionation in the slow solar wind, *Astrophys. J. 521*, 859-867, 1999.

Von Steiger, R., J. Geiss, and G. Gloeckler, Composition of the solar wind, in *Cosmic Winds and the Heliosphere*, edited by J.R. Jokipii, C.P. Sonett, and M.S. Giampapa, pp. 581-616, Univ. of Ariz. Press, Tucson, 1989.

Wang, Y.-M., Element separation by upward proton drag in the chromosphere, *Astrophys. J. 464*, L91-L94, 1996.

P. Bochsler, J. M. Weygand, and P. Wurz, Physikalisches Institut, University of Bern, Sidlerstrasse 5, CH 3012 Bern, Switzerland. (Peter.Bochsler@phim.unibe.ch)

F. M. Ipavich and J. A. Paquette, Department of Physics, University of Maryland, College Park, MD 20742. (Ipavich@umtof.umd.edu)

(Received September 6, 1999; revised November 19,1999; accepted December 9, 1999.)